CHEMISTRY
A EUROPEAN JOURNAL

DOI: 10.1002/chem.200600709

Proton Walk in the Aqueous Platinum Complex [TpPtMeCO] via a Sticky σ-Methane Ligand

H. Christine Lo,[b] Mark A. Iron,[a, d] Jan M. L. Martin,*[a] and Ehud Keinan*[b, c]

Abstract: Both experimental and theoretical evidence suggest that the proton exchange between water and the methyl group in [TpPt(CO)CH_3] (**1**, Tp = hydridotripyrazolylborate) involves the formation and deprotonation of a "sticky" σ-methane ligand. The efficiency of this nontrivial process has been attributed to the spatial orientation of functional groups that operate in concert to activate a water molecule and then achieve a multistep proton walk from water to an uncoordinated pyrazolyl nitrogen atom, to the methyl ligand, and then back to the nitrogen atom and water. The overall proton-exchange process has been proposed to involve an initial attack of water at the CO ligand in **1** with concerted deprotonation by the uncoordinated pyrazolyl nitrogen atom. The pyrazolium proton is then transferred to the Pt–CH_3 bond, leading to a σ-methane intermediate. Subsequent rotation and deprotonation of the σ-methane ligand, followed by reformation of **1** and water, result in scrambling of the methyl protons with the hydrogen atoms of water. An alternative two-step process that involves oxidative addition and reductive elimination has also been considered. The two competing mechanistic routes from **1** into [D_3]-**1**, as well as the conversion of **1** into [TpPt(CH_3)H_2] (**2**), have been examined by density functional theory (DFT) using a variety of exchange-correlation methods, primarily PW6B95, which was recently shown to be highly accurate for evaluating reactions of late-transition-metal complexes. The key role played by the free pyrazolyl nitrogen atom, acting as a proton carrier that abstracts a proton from water and transfers the proton to the Pt–CH_3 bond, is reminiscent of the dual functionality of histidine in the catalytic triad of natural serine proteases.

Keywords: methane complexes · alkanes · hydrogen transfer · platinum · proton exchange

Introduction

Nature meets difficult chemical challenges, such as the deprotonation of high-pK_a species and activation of inert bonds under mild conditions, through the meticulous spatial positioning of protein functional groups that operate in concert. A well-studied example of such polyfunctional machinery is the catalytic triad, which shuttles protons from water consecutively through three protein residues and back to water.[1] Application of Nature's strategies to nonbiological domains could lead to the catalysis of demanding chemical transformations. Of particular significance is the domain of transition-metal chemistry, in which diverse oxidation states and rich coordination geometries provide metal atoms not only with catalytic properties, but also with the ability to orchestrate the relative orientation and chemical cooperativity of several functional groups within its coordination sphere.

An important class of difficult chemical reactions is the functionalization of saturated hydrocarbons. Selective methane oxidation by transition metals has been a major challenge in chemistry and a target of extensive experimental

[a] Dr. M. A. Iron, Prof. Dr. J. M. L. Martin
Department of Organic Chemistry
Weizmann Institute of Science
Rehovot, 76100 (Israel)
E-mail: comartin@wicc.weizmann.ac.il

[b] Dr. H. C. Lo, Prof. Dr. E. Keinan
Department of Molecular Biology and
The Skaggs Institute for Chemical Biology
The Scripps Research Institute
10550 N. Torrey Pines Rd., La Jolla, CA 92037 (USA)
E-mail: keinan@tx.technion.ac.il

[c] Prof. Dr. E. Keinan
Schulich Faculty of Chemistry and Institute of Catalysis, Science and Technology
Technion–Israel Institute of Science
Haifa 32000 (Israel)

[d] Dr. M. A. Iron
Current address: Department of Chemistry, University of Minnesota
Minneapolis, MN 55455-0431 (USA)

Supporting information for this article is available on the WWW under http://www.chemeurj.org/ or from the author.

and theoretical efforts.[2–10] Nevertheless, mechanistic understanding of the methane C–H activation process in the very few successful cases remains inconclusive.[2,3] A possible deprotonation of a σ-methane metal complex has been proposed in parallel with the deprotonation of its isomeric methyl hydride (methanido hydrido) complex.[3,5] Although the direct deprotonation of metal hydridoaryl complexes[11–13] and of a metal dihydrogen complex[14–19] is known, no clear evidence for deprotonation of a σ-alkane ligand is available.

We recently reported that [TpPt^{II}Me(CO)] (**1**, Tp = hydridotripyrazolylborate) reacts with H_2O to form the thermally and air-stable complex [TpPt^{IV}Me(H)$_2$] (**2**), which equilibrates rapidly with [TpPt^{II}H(σ-CH$_4$)] in solution without liberation of either methane or dihydrogen even at elevated temperatures.[20,21] We attributed the thermal stability of **2** to the rigidity of the Tp ligand which prevents *trans* coordination of two pyrazolyl rings.[22] The transitory formation of a σ-methane complex was supported by computational studies and by the observation that when **2** was dissolved in a deuterated protic solvent, such as [D$_4$]methanol, D_2O/[D$_8$]THF, or D_2O/[D$_6$]acetone, only [D$_5$]-**2** was produced.

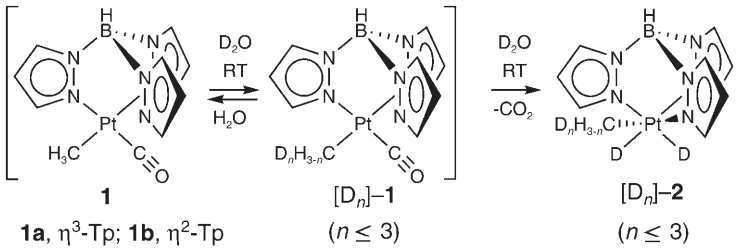

Scheme 1. H/D scrambling in **1** and its conversion into **2**.

Herein we show that when complex **1** is dissolved in a mixture of D_2O and an organic solvent, its methyl ligand surprisingly undergoes H/D exchange prior to its complete conversion into **2** (Scheme 1). This transformation is clearly identified by the observation of [D$_1$]-**1** and [D$_2$]-**1** isotopologues in the ^{1}H NMR spectra of the reaction mixture, as well as **2** and its isotopologues. We propose that these results could be interpreted in terms of a three-station proton walk mechanism.[23] The observed experimental results and conclusions are compared with a computational study conducted using density functional theory (DFT) methods.

Results and Discussion

When **1** was dissolved in either D_2O/[D$_8$]THF or D_2O/[D$_6$]acetone, the isotopologues [D$_1$]-**1** and [D$_2$]-**1** were observed by ^{1}H NMR spectroscopy along with **2**, [D$_1$]-**2**, and [D$_2$]-**2** (Figure 1).[24] In principle, H/D scrambling in **1** can proceed directly from **1** or by the reverse transformation of **2** into **1**. The latter option cannot be excluded since CO_2 insertion into M–H bonds is known to lead to metal formate

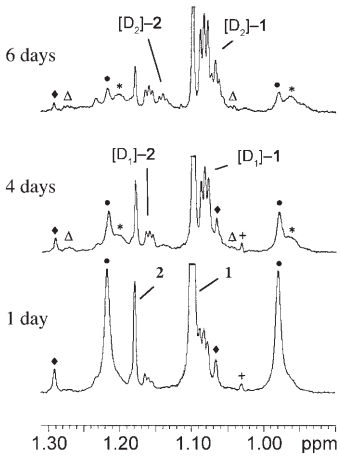

Figure 1. ^{1}H NMR spectra (300 MHz, 1:1 D_2O/[D$_6$]acetone) showing H/D exchange at the methyl ligand of **1**: [D$_1$]-**1** appears as a 1:1:1 triplet and [D$_2$]-**1** as a 1:2:3:2:1 quintet. $\Delta\delta[D1] = \delta(CH_3) - \delta(CDH_2) = 0.016$ ppm; $\Delta\delta[D2] = \delta(CH_3) - \delta(CD_2H) = 0.031$ ppm; $^2J_{H,D} = 1.5$ Hz; digital resolution = 0.069 Hz/point. All complexes show ^{195}Pt (natural abundance 33.8%) satellite couplings. (●) Satellite coupling of **1**; (◆) satellite coupling of **2**; (*) satellite coupling of [D$_1$]-**1**/[D$_2$]-**1**; (△) satellite coupling of [D$_1$]-**2**/[D$_2$]-**2**; (+) spinning side band of **1**, symmetrically disposed. Owing to the poor solubility of **2**, some of it precipitated in the NMR tube. Also, the vertical scales of these spectra were not normalized.

Abstract in Hebrew:

העבודה המתוארת כאן, מציגה ראיות ניסויות ותיאורטיות, אשר תומכות בהשערה כי חילוף הפרוטונים בין מים לבין הליגנדה המתילית בקומפלקס $TpPt(CO)CH_3$ (**1**, Tp = הידרידוטריספירזולילבוראט) מתרחש תוך כדי יצירה ודה-פרוטונציה של ליגנדת סיגמה-מתאן "דביקה". יעילותו של התהליך המורכב הזה, אשר גורם להפיכתו של **1** ל-**1**-d_3, מיוחסת לאירגון המרחבי של הקבוצות הפונקציונליות סביב אטום המתכת. שיתוף הפעולה בין הקבוצות האלה גורם לשיפעול מולקולת מים, אשר גורם לשרשרת אירועים של מעבר פרוטון מהמים אל אטום החנקן בקבוצת הפירזוליל שאיננה קשורה למתכת, משם אל הליגנדה המתילית, וממנה חזרה לאטום החנקן ולמולקולת המים. המנגנון המוצע של התהליך הזה מתחיל בהתקפה נוקלאופילית של מולקולת מים משופעלת על הליגנדה הקרבונילית בקומפלקס **1**. השפעול מתבצע ע"י מעבר פרוטון ממולקולת המים הזאת אל אטום החנקן בקבוצת הפירזוליל הבלתי קשורה. לאחר מכן נודד הפרוטון מאטום החנקן אל קבוצת המתיל ובאופן כזה נוצרת ליגנדת סיגמה-מתאן "דביקה". סבוב של ליגנדת המתאן סביב הקשר, המחבר אותה למתכת, ולאחר מכן החזרת פרוטון אחר מהמתיל אל אטום החנקן ומשם למים, גורמים בסופו של דבר לחילוף כל הפרוטונים בקבוצת המתיל של קומפלקס **1** עם אלו של המים. המנגנון הנ"ל, המנגנון האלטרנטיבי, אשר כולל שלבים של סיפוח מחמצן ואלימינציה מחזרת, וכן תגובת ההמשך במים, שבה **1** הופך לקומפלקס **2**, $TpPt(CH_3)H_2$, נחקרו כולם בשיטות חישוביות, כגון DFT ושיטות שונות של חילוף-קורלציה, בעיקר שיטת PW6B95, אשר הוכחה לאחרונה כשיטה מדויקת מאד לחישוב תגובות של קומפלקסי מתכות מעבר מאוחרות. תפקיד המפתח של קבוצת הפירזוליל הבלתי קשורה למתכת, כמעבירה פרוטונים הלוך וחזור, מהמים אל הקשר פלטינה-מתיל, מזכיר את פעולתה הכפולה של קבוצת ההיסטידין בשילוש הקטליטי, אשר קיים בטבע באנזימים ממשפחת הפרוטאזות הסריניות.

complexes.[25] In order to examine this possibility, two freeze–pump–thaw cycles were carried out every 12 h to remove any CO_2 generated in the reaction of **1** with D_2O. This procedure, however, did not affect the H/D exchange rate. Furthermore, when a solution of **2** in either D_2O/[D_8]THF (1:1) or D_2O/[D_6]acetone (1:1) was kept under CO_2 (1 atm, room temperature) for more than a week, only [D_5]-**2** was formed, but neither **1** nor any other complex could be detected by ^1H NMR spectroscopy. Consequently, **2** is not involved in the H/D exchange reaction in **1**.

A direct proton transfer or a multistep mechanism? H/D scrambling in **1** thus likely occurs via a σ-methane intermediate[26] prior to the loss of CO_2. Two mechanistic routes are possible for the formation of a σ-CH_4 intermediate in aqueous solutions of **1**. Intuitively, this intermediate could be formed by either direct protonation at the methyl ligand by the solvent or by protonation at the metal to form a metal hydride followed by reductive coupling of the methyl and hydride ligands. A less trivial, multistep mechanism could involve the other ligands. To check whether these intuitive options are possible, the reactivity of **1** in protic media was compared with that of the isoelectronic analogues **3**–**5**. When complexes **3** and **4**, in which the CO is replaced by an electron-withdrawing and an electron-donating

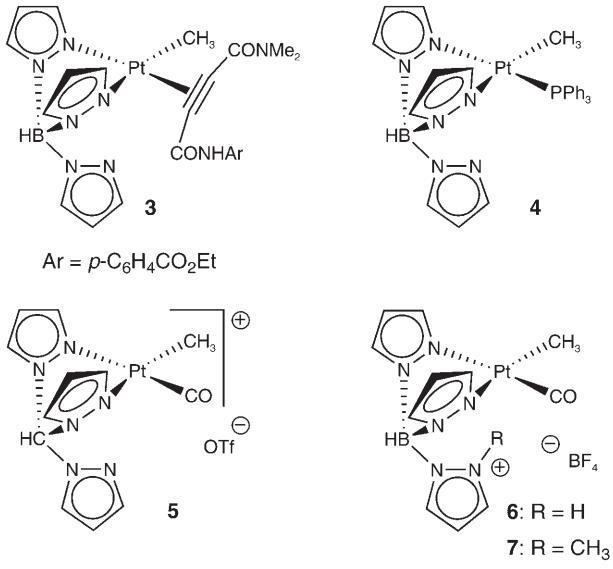

ligand, respectively, were heated at 55 °C for two days in either D_2O/[D_8]THF (1:1) or D_2O/[D_6]acetone (1:1), H/D exchange products were not detected. The tripyrazolylmethane (TpC) complex **5** is a cationic, isoelectronic analogue of **1**. Although cationic, electron-deficient complexes are expected to undergo slower protonation than their neutral analogues, the H/D exchange in **5** was found to be much faster than that in **1** under the same conditions (Figure 2). These findings disfavor a mechanism of direct protonation/deprotonation at either the methyl ligand or the metal center. Furthermore, they highlight the crucial role of the Tp and CO ligands in the H/D exchange reaction.

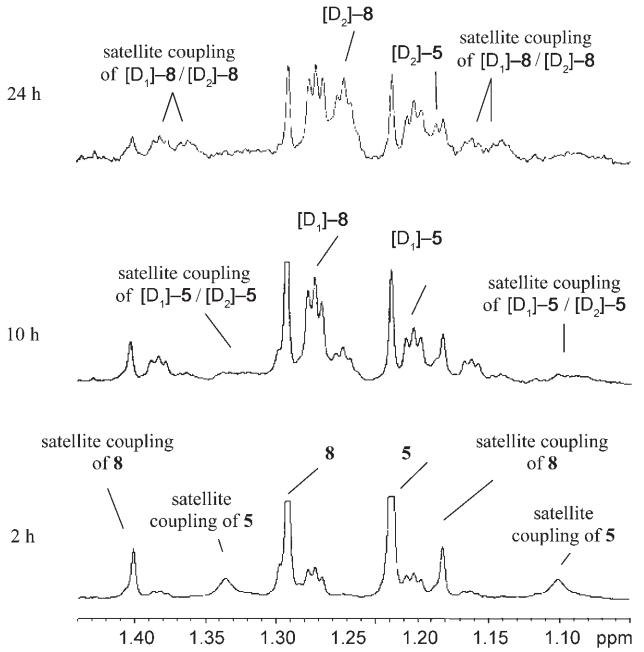

Figure 2. The ^1H NMR spectra (300 MHz, 1:1 D_2O/[D_6]acetone) for H/D exchange at the methyl ligand in **5**, showing [D_1]-**5** and [D_2]-**5**, with [D_1]-**5** exhibiting a triplet (1:1:1) and [D_2]-**5** a quintet (1:2:3:2:1). $\Delta\delta[D1] = \delta(CH_3) - \delta(CDH_2) = 0.016$ ppm; $\Delta\delta[D2] = \delta(CH_3) - \delta(CD_2H) = 0.031$ ppm; $^2J_{H,D} = 1.5$ Hz; digital resolution = 0.069 Hz/point. All complexes show ^{195}Pt (natural abundance, 33.8%) satellite couplings. Complex **8** is [(TpC)Pt$(H)_2CH_3$]OTf.

Therefore, it is apparent that the observed H/D exchange in **1** originates from a multistep mechanism. We propose a mechanism that commences with a nucleophilic attack by water on the carbonyl to give a hydroxycarbonyl complex, **B** (Scheme 2). Electron-deficient metal carbonyls are known to be susceptible to reversible nucleophilic attack by activated water, resulting in the formation of electron-rich metal hydroxycarbonyls.[27–29] The reversible nature of similar reactions was demonstrated by carbonyl oxygen exchange with $H_2{}^{18}O$.[27,28] The carbonyl in **1**, especially in the η^2-Tp form, **1b**, observed by X-ray crystallography,[30] is electron-deficient and thus nucleophilic attack is conceivable. Moreover, the nitrogen atom of the pendant pyrazolyl ring is well situated to activate a water molecule for concerted attack on the CO ligand, as shown in **A**. The structure of **B** is supported by related reports[31,32] and by our previous observation that **1** is quantitatively converted into **6** under acidic conditions.[20]

Possible reaction pathways: Scheme 2 presents three possible pathways for the formation of a σ-CH_4 intermediate from **B**. One could envision that **B**, which bears two acidic protons, could lead to the σ-methane complexes **C** or **D** via transition state **TS(B-C)** or **TS(B-D)**. Each transition state features a weak interaction between the Pt–Me bond and either the pyrazolium or the carboxy proton, respectively. In addition, the oxidative addition product, **E**, could also be an

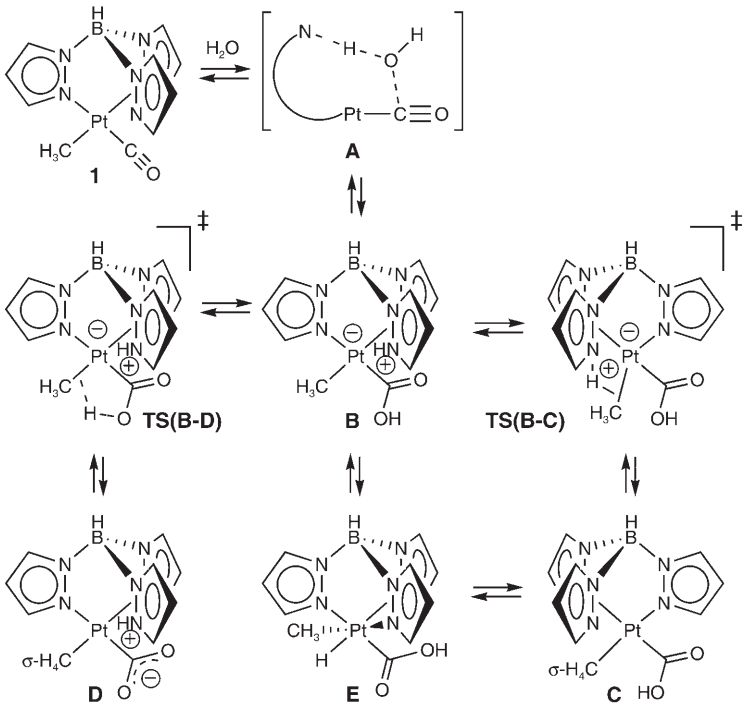

Scheme 2. Possible routes for H/D exchange in **1**.

intermediate on the way from **B** to **C** through two reversible redox transformations.

It is hard to determine which route is preferred. In a closely related theoretical study of the Shilov system, the deprotonation of a $Pt^{II}(\sigma\text{-}CH_4)$ and its $Pt^{IV}Me(H)$ isomer was found to be competitive.[33,34] Furthermore, on the basis of population analyses of stable Pt^{IV} complexes, it has been suggested that both Pt^{IV}–H and Pt^{IV}–CH_3 are best described as covalent bonds,[35] indicating a higher energy barrier for deprotonation of the Pt–H bond in **E**. On the other hand, complexes **B** and **E** could represent the possible protonation products of **1** in acidic aqueous solution. As protonations at nitrogen and oxygen atoms are often kinetically favored whereas metal protonation is thermodynamically favored,[36] the routes represented by **TS(B-C)** and **TS(B-D)** could be preferred over **E**. A more thermodynamically stable intermediate **E**, relative to **B**, would result in a high activation energy for the back reaction in a reversible process.

To gain a better understanding of the H/D exchange mechanism in **1**, we carried out the reaction at different temperatures in the hope of detecting a reaction intermediate. Solutions of ^{13}C-labeled **1** in either H_2O/[D_6]acetone (1:1) or D_2O/[D_6]acetone (1:1) were kept at 20, 10, 0, and −20 °C and monitored over a period of eight hours by $^{13}C\{^1H\}$ NMR spectroscopy.[24a] Remarkably, the $^{13}CO_2$ signal was observed in all of the reaction mixtures, including the one at −20 °C in D_2O/[D_6]acetone. However, signals other than those associated with **1** and **2** could not be detected. The ^1H NMR spectra of these mixtures, taken after the ^{13}C NMR monitoring period, showed small amounts of [D_1]-**1** and [D_2]-**1**, particularly at the higher temperatures. Even at −20 °C, a very weak 1:1:1 triplet corresponding to [D_1]-**1** was detected. Our inability to observe stable intermediates, such as **E**, might suggest that H/D exchange might occur via an intramolecular σ-bond metathesis mechanism,[34] as described in **TS(B-C)** and **TS-(B-D)**. Nevertheless, the mechanistic route involving **E** cannot be excluded.

The role of the uncoordinated pyrazolyl nitrogen atom as a proton carrier: The role of the uncoordinated pyrazolyl ligand in the H/D exchange in **1** was revealed by the reactivity of the cationic complexes **6** and **7**, in which the nitrogen atom of the uncoordinated pyrazolyl ring is unavailable as a free base. When **6** was dissolved in either D_2O/[D_8]THF (1:1) or D_2O/[D_6]acetone (1:1), neither H/D exchange at the methyl ligand nor methane liberation could be observed by ^1H NMR spectroscopy, even after three months at room temperature. Only [D_1]-**6** and free pyrazole were formed in these mixtures along with some black precipitate. The same result was observed when **6** was generated in situ from **1** and HBF_4 (1.0–1.5 equiv). Likewise, a very similar outcome was obtained when **7** was kept in either D_2O/[D_6]acetone (1:1) or CD_2Cl_2 saturated with D_2O for a week.

It could be argued that H/D exchange does not occur in complexes **6** and **7** because their carbonyl ligands are not susceptible to nucleophilic attack by water. To examine this issue, oxygen-exchange experiments with $H_2{}^{18}O$ were performed. ^{13}CO-labeled complexes, **1**, **5**, **6**, and **7**, were dissolved in $H_2{}^{18}O$/[D_6]acetone and the ^{18}O isotope-induced shift[37] in the $^{13}C\{^1H\}$ NMR spectra was monitored (Figure 3). All four carbonyl complexes exhibited moderate-to-slow oxygen exchange with $H_2{}^{18}O$, thus indicating that these complexes do indeed undergo nucleophilic attack by water. In agreement with their higher electron deficiencies,[27–29] the cationic complexes **5**, **6**, and **7** exhibited much faster oxygen exchange than **1** (relative rates: $\mathbf{1} < \mathbf{5} \approx \mathbf{6} < \mathbf{7}$).

The observation that complexes **6** and **7** undergo oxygen exchange with water, but neither H/D exchange at the methyl group nor methane liberation indicates that their hydroxycarbonyl intermediates can be formed, but their σ-methane intermediates cannot. It has been demonstrated that in the absence of a base, the equilibrium between metal carbonyls and metal hydroxycarbonyls lies heavily towards the former.[29] Accordingly, the above results can be interpreted in terms of a fast equilibrium between the carbonyls

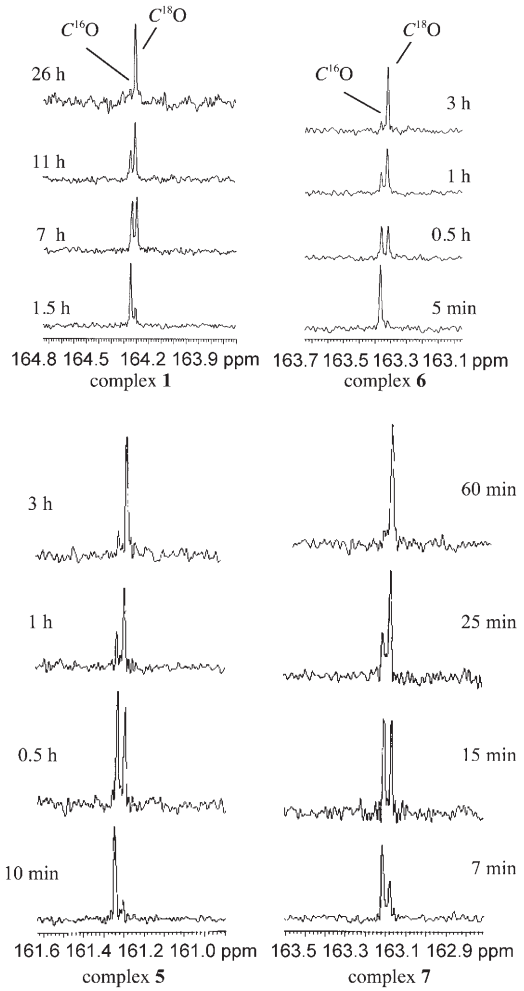

Figure 3. $^{13}C\{^1H\}$ NMR spectra (75.5 MHz) showing $^{16}O/^{18}O$ exchange of the carbonyl ligand of **1** and **6** (top) and **5** and **7** (bottom) in 0.8 mL [D_6]acetone and 100 μL of $H_2{}^{18}O$. $\Delta\delta = \delta(C^{16}O) - \delta(C^{18}O) = 0.035$–$0.038$ ppm; pulse width = 30°; delay time, $d_1 = 0.5$ s; number of transients, ns = 32; digital resolution = 0.38 Hz/point, with a line broadening of 0.3 Hz. The signals due to ^{195}Pt satellite couplings are not shown.

and hydroxycarbonyls with very low steady-state concentrations of the latter, thus preventing the formation of the σ-methane intermediate. We suggest that the uncoordinated pyrazolyl nitrogen atom in **1** and **5** serves as a base that stabilizes the hydroxycarbonyl intermediate. This pyrazolyl nitrogen atom probably acts as a proton shuttle that takes a proton from water, delivers it to the methyl group, and carries out the reverse sequence, thus exhibiting dual functionality as both a base and an acid. These considerations make the mechanistic route involving **TS(B-D)**, which does not require the involvement of a free pyrazolyl ligand, less likely than the one via **TS(B-C)**.

The structure of the transition state **TS(B-C)**, featuring a zwitterionic, three-atom hydrogen-bonding $N^+{-}H{\cdots}CH_3{-}Pt^{II-}$ moiety, is supported by the crystallographic data of a zwitterionic platinum(II) complex reported by van Koten and co-workers.[38] In that complex, a bridging proton was found to point towards the middle of the Pt–Br bond, exhibiting a strong $N^+{-}H{\cdots}Br{-}Pt^{II-}$ electrostatic interaction, with the N–H bond being longer than usual (0.98 Å).[38,39] This three-atom hydrogen bond was also manifested by the lack of spin–spin couplings between the proton and either the ^{15}N or ^{195}Pt nucleus. In marked contrast, such couplings are observed in all zwitterionic $Pt^{II-}{\cdots}H{-}N^+$ complexes in which the proton bridges only two atoms, platinum and nitrogen, with the N–H bond length being 0.88 Å.[39]

The high electron density in **B** could encourage proton transfer from the pyrazolium site to the Pt–Me bond via **TS-(B-C)**. In contrast, an analogous transformation in electron-deficient carbonyl complexes via **TS(B-C)′** would be less favorable. Indeed, dissolving **1** in dry CD_3CO_2D to produce

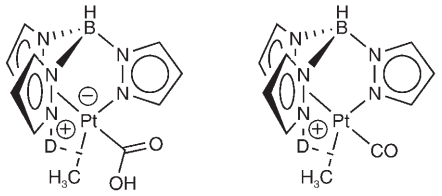

[D_1]-**6** and keeping it for over three weeks at room temperature did not lead to any observable reaction by ^1H NMR spectroscopy, indicating that neither H/D exchange nor methane liberation occurred under these conditions. This observation is consistent with the notion that the Pt–Me bond in **6** is too electron-deficient to be protonated. We also conclude from this observation that even if formation of the σ-methane intermediate ever took place in **6** under these conditions, H/D exchange would not occur because the pyrazolium nitrogen atom is no longer available as a base for the deprotonation step. The efficient proton exchange between the uncoordinated pyrazolyl nitrogen atom and the Pt–Me bond in **1** and **5** may reflect similar Lewis basicity of these two sites. A similar proposal has been made for an equilibrium between a metal hydride and its tautomer.[11]

NMR and ESI-MS evidence for the formation of a σ-methane ligand in 5: Experiments with the TpC complex **5** provided evidence for the existence of a σ-methane intermediate during the H/D exchange reaction. Small amounts of CH_3D and CH_2D_2 were identified by ^1H NMR spectroscopy in a solution of **5** in D_2O/[D_6]acetone (1:1) (Figure 4). As [(TpC)Pt(H)$_2$CH$_3$]OTf (**8**) (an analogue of **2**), is also produced in aqueous solutions of **5** (the analogue of **1**), we carried out the same reaction with **8** at room temperature for 24 h, but no free methane could be observed in the mixture. Clearly, the observed CH_3D and CH_2D_2 resulted from the reaction of **5** with D_2O, but not from **8**.

Moreover, ESI-MS revealed a new compound (*m*/*z* 472) in the solution of **5** (*m*/*z* 452) in H_2O/acetone (1:1 to 3:1) (Figure 5). The mass of the new peak at *m*/*z* 472, the intensity of which increased with increasing water concentration in the solvent, is consistent with the formula [(TpC)Pt(CO_2H)-

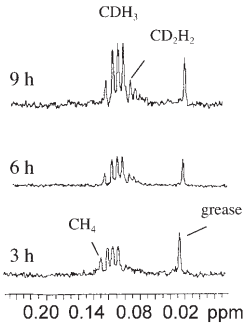

Figure 4. ^{1}H NMR spectra (300 MHz, D_2O/[D_6]acetone, 1:1) of **5** exhibiting CDH_3 and CD_2H_2 as a 1:1:1 triplet and a 1:2:3:2:1 quintet, respectively. $\Delta\delta[D1]=\delta(CH_4)-\delta(CDH_3)=0.015$ ppm; $\Delta\delta[D2]=\delta(CH_4)-\delta(CD_2H_2)=0.031$ ppm; $^2J_{HD}=2.0$ Hz. The observed trace amounts of CH_4 could result from residual DHO present in D_2O.

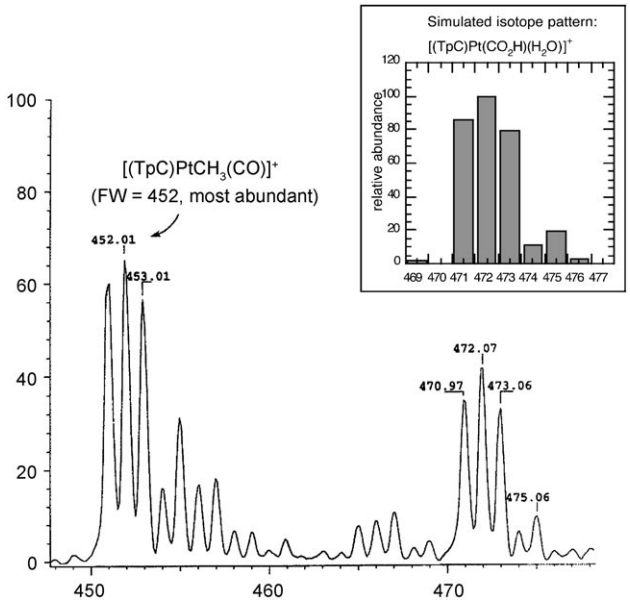

Figure 5. ESI-MS spectrum of **5** in H_2O/acetone (1:1 ≈3:1), along with a computer simulated isotope distribution pattern (inset) of [(TpC)Pt-$(CO_2H)(H_2O)]^+$ (**8**). The mass spectrometer was set to detect positively charged mass ions.

$(H_2O)]^+$. We suggest that displacement of the σ-methane ligand in **C′** by water (Scheme 3) results in the formation of this aqua complex $[(TpC)Pt(CO_2H)(H_2O)]^+$.

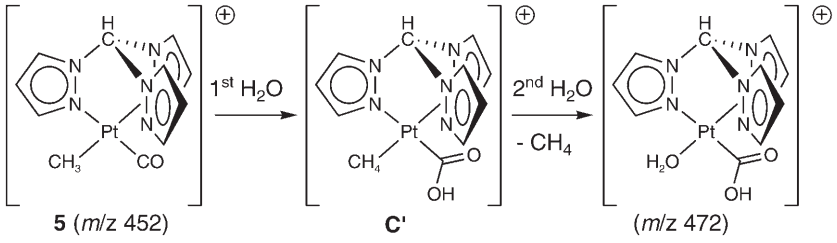

Scheme 3.

Based on these experiments we conclude that a σ-methane intermediate also exists in an aqueous solution of **1**. In a control experiment, saturating a solution of **1** in H_2O/[D_8]THF (1:1) with CD_4 did not lead to any detectable free CH_4 or its isotopologues even after two weeks at room temperature. We thereby conclude that the σ-methane ligand is more tightly bound in **1** than in **5**.

DFT mechanistic study: To better understand the exchange mechanism, density functional theory (DFT) calculations were performed on the system at a number of levels of theory. The data in Table 1 allows comparison of the results obtained at each level. For the purposes of the following discussion, the COSMO(H_2O)-PW6B95/SDB-cc-pVTZ//PW6B95/SDD results are considered although the other levels yield similar conclusions (see Table 1). The PW6B95 results were chosen for the discussion since a recent study showed that this functional, of all those tested, was the most reliable for calculations involving transition-metal complexes and associated reaction barriers.[40] Figure 6 depicts the structures of all the calculated complexes and Figure 7 illustrates the energy profiles of the proposed pathways shown in Scheme 2 and Scheme 4 below. (The reaction profiles at the other levels of theory are included in the Supporting Information.) Based on the results presented in Table 1, Figure 7, and the Supporting Information, one notes that one would make similar conclusions with the other functionals.

These calculations show that complex **1** prefers the η^2-Tp mode, **1b**, over the η^3-Tp mode, **1a**, by $\Delta G_{298}=5.2$ kcal mol^{-1}. It is known that Pt^{II} complexes generally prefer 16-electron square-planar over 18-electron pentacoordinate complexes, and this geometric preference is supported by an X-ray crystallographic study.[30] A water-coordination complex **A** was found in which a water molecule is hydrogen-bonded to the free pyrazolyl nitrogen atom. The formation of this complex is endergonic. Activation of the O–H bond in water via **TS(A-B$_1$)** involves an overall barrier of $\Delta G^{\ddagger}_{298}=24.7$ kcal mol^{-1}, leading to complex $\mathbf{B_1}$ with an N···H–O hydrogen bond. Two other similar complexes were found and all three are of a similar energy. In complex $\mathbf{B_2}$ the COOH moiety is rotated and in complex $\mathbf{B_3}$ the hydrogen bridges the pyrazolyl nitrogen atom and the platinum center. Such a complex is not unprecedented and resembles a zwitterionic $Pt^{II-}\cdots H-N^+$ moiety, observed by NMR and X-ray crystallography to have a proton bridging the platinum and nitrogen centers.[38] A similar complex has an NH proton directed towards the middle of a Pt–Br bond (vide supra).[38] The barriers to the interconversions of $\mathbf{B_1}$, $\mathbf{B_2}$, and $\mathbf{B_3}$ are not expected to be significant, especially in a protic solvent.

The key mechanistic question is which of the three H/D

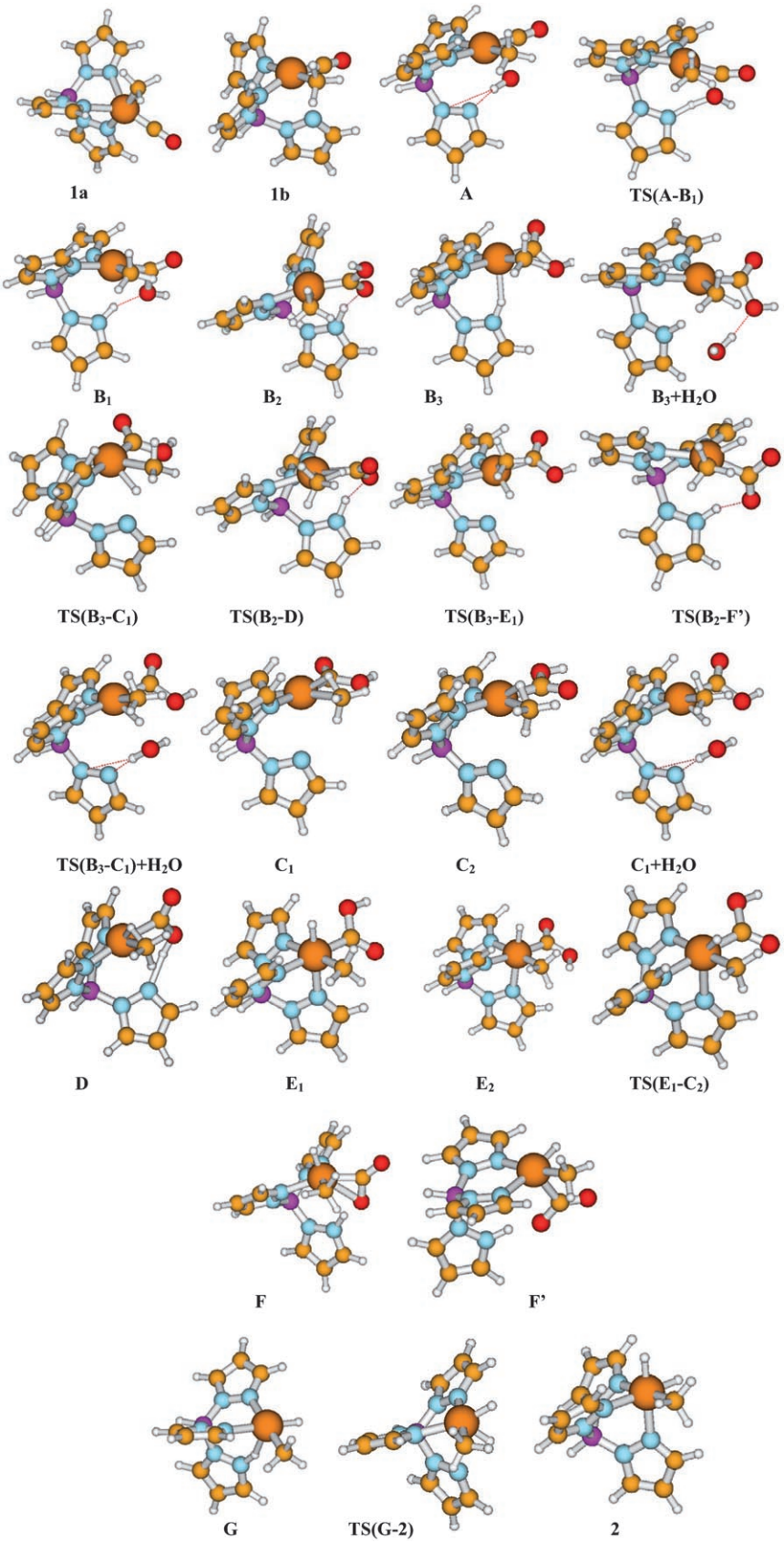

Figure 6. Calculated structures (PW6B95/SDD) of the intermediates and transition states involved in H/D exchange in **1** and its conversion into **2**. Note that in **A**, the second hydrogen of the water molecule is obscured by the oxygen atom. (Color code: C: brown; H: white; Pt: orange; N: blue; O: red; B: purple.)

exchange pathways discussed above is the most plausible. Calculations show that the barrier to proton transfer from the pyrazolyl nitrogen atom to the methyl group, **TS(B_3-C_1)**, is $\Delta G^{\ddagger}_{298} = 29.8$ kcal mol^{-1}, and this step has a reaction energy of $\Delta G_{298} = 14.5$ kcal mol^{-1}. The barrier to **TS(B_2-D)**, in which the proton is transferred from the carboxy group, is slightly higher ($\Delta G^{\ddagger}_{298} = 30.7$ kcal mol^{-1}). The third potential pathway is an oxidative addition/reductive elimination route from $\mathbf{B_3}$ via $\mathbf{E_1}$ to $\mathbf{C_2}$ (which differs from $\mathbf{C_1}$ in the orientation of COOH). This route entails two barriers, **TS(B_3-E_1)** with $\Delta G^{\ddagger}_{298} = 27.2$ kcal mol^{-1} and **TS(E_1-C_2)** with $\Delta G^{\ddagger}_{298} = 23.8$ kcal mol^{-1}.

The reaction was carried out in a protic medium (i.e., water), and thus participation of a second water molecule in the H/D scrambling process is also possible. Complexes $\mathbf{B_3 + H_2O}$ and $\mathbf{C_1 + H_2O}$ were optimized, along with the associated transition state. Although the additional water molecule somewhat destabilizes complexes $\mathbf{B_3}$ and $\mathbf{C_1}$, the overall barrier height does not change significantly.

Regardless of by which pathway the reaction proceeds, the effective barrier to the reaction would be the relative energy of the highest transition state. **TS(B_3-E_1)** and **TS(E_1-C_2)** are clearly lower than any of the single-step reactions. It is thus reasonable to assume that the σ-methane complex is generated via a two-step oxidative addition/reductive elimination mechanism rather than a concerted proton transfer. From our previous work on H/D exchange in **2**,[22] we know that the barrier for the rotation of coordinated methane is on the order of a few kcal mol^{-1}, which is less than the reverse barrier from $\mathbf{C_2}$ ($\Delta G^{\ddagger}_{298} = 8.1$ kcal mol^{-1}),

Table 1. Computed relative energies [kcal mol^{-1}] for all the complexes in the DFT study at different levels of theory.[a] Unless indicated otherwise, all energies were calculated using the PW6B95/SDD geometries and the SDB-cc-pVTZ basis set, and include bulk solvent affects (COSMO).

Geometry	PW6B95	B1B95	PBE0	BMK// BMK[b]	BMK/ DZ[b,c]	B971// BMK[b]	τ-HCTHh/DZ// BMK[b,c]	mPW1K/ DZ[c,d]	B97-1/DZ// mPW1K[c,d]
1a	5.2	4.8	4.5	4.6	3.9	4.7	2.4	4.0	4.0
1b	0.0	0.0	0.0	0.0	0.0	0.0	0.0	0.0	0.0
A	5.4	7.4	6.1	6.0	3.4	6.1	2.7	6.0	4.5
TS(A-B1)	24.7	25.9	22.4	25.5	19.2	23.1	14.1	19.5	18.3
B1	12.0	13.2	10.3	13.5	7.9	13.1	5.4	5.1	6.5
B2	9.9	10.8	7.8	11.8	6.4	11.6	3.9	1.9	4.1
B3	8.3	9.2	5.0	10.2	4.8	8.8	1.0	1.8	2.9
B3+H_2O	13.5	17.6	12.8	15.7	6.2	15.1	3.0	NR[e]	NR
TS(B3-C1)	38.1	38.3	34.7	41.6	35.5	33.1	32.2	33.4	34.2
TS(B3+C1)+H_2O	38.5	40.6	33.9	41.3	29.9	39.8	24.7	NR	NR
TS(B2-D)	40.6	41.1	38.0	43.6	38.6	43.1	33.8	39.8	39.8
TS(B3-E1)	35.6	36.4	33.0	32.9	25.9	34.1	25.3	27.5	25.9
TS(B2-F′)	44.3	44.5	40.2	47.2	NR	NR	NR	NR	NR
C1	22.8	24.3	22.4	22.8	18.0	25.3	19.3	17.1	19.1
C2	23.4	24.9	23.1	23.9	19.1	26.3	20.3	17.4	19.3
C1+H_2O	29.4	32.7	28.4	31.5	22.4	32.8	21.6	NR	NR
D	18.0	19.3	17.3	20.8	16.0	21.6	14.6	16.1	17.8
E1	7.7	8.2	4.8	4.0	−2.5	9.8	−0.5	−0.6	1.1
E2	8.8	9.2	6.0	5.2	−1.0	10.7	0.7	3.0	4.6
TS(E1-C2)	31.5	32.0	28.8	31.8	25.3	32.4	23.2	24.0	25.5
F	30.1	30.9	26.7	30.8	24.8	31.1	20.4	24.3	21.1
F′	16.8	18.1	13.1	14.1	NR	NR	NR	NR	NR
G	1.3	1.0	−0.1	5.2	0.7	1.8	−5.8	−2.5	−4.4
TS(G-2)	13.4	13.1	12.8	11.1	6.4	12.3	5.9	14.1	10.4
2	−4.9	−5.0	−5.3	−7.6	−12.9	−3.5	−12.8	−10.0	−10.8

[a] Energies measured relative to **1b** as zero reference. [b] The BMK/SDD geometries were employed in the energy calculations. [c] The SDB-cc-pVDZ basis set was employed in the energy calculations. [d] The mPW1K/SDD geometries were employed in the energy calculations. [e] Calculations not carried out.

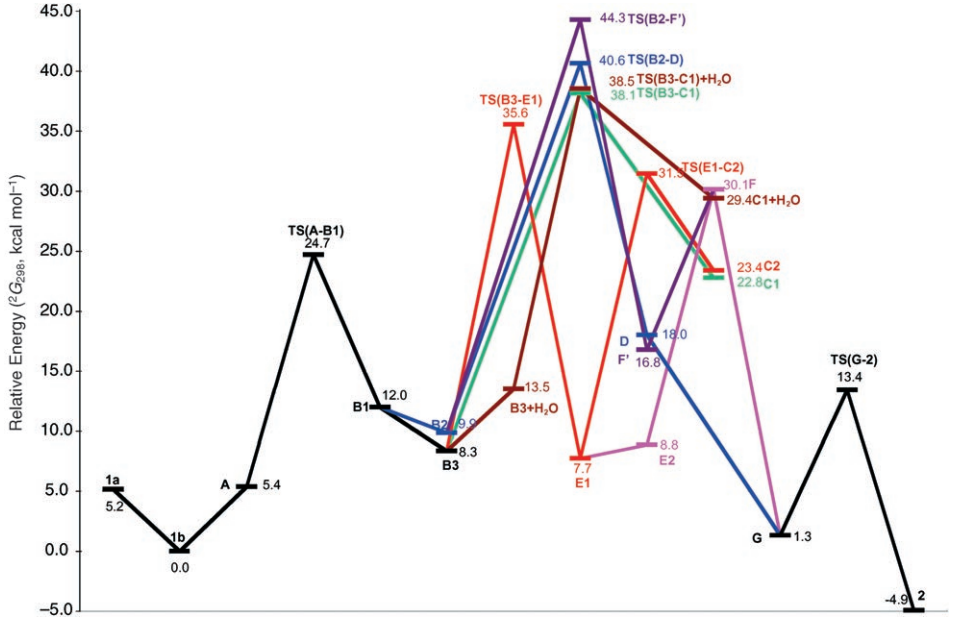

Figure 7. Reaction profiles (ΔG_{298} [kcal mol^{-1}], COSMO(H_2O)-PW6B95/SDB-cc-pVTZ//PW6B95/SDD) of the different possible reaction profiles for H/D scrambling in **1** and its conversion into **2**. (Color key: black, mechanism common to all possible profiles; green, H/D exchange via $\mathbf{C_1}$; blue, H/D exchange via **D** and conversion into **2**; maroon, H/D exchange via $\mathbf{C_1}$ assisted by H_2O; red, H/D exchange via $\mathbf{E_1}$ and $\mathbf{C_2}$; pink, formation of **2** via $\mathbf{E_1}$ and **F**; purple, formation of **2** by direct deprotonation of the COOH moiety).

thereby allowing for H/D exchange via the σ-methane complex. Likewise, methane loss from any of the σ-methane complexes is unlikely for similar reasons as methane loss from **2** is not observed, specifically the rigidity of the Tp ligand and the resulting high energy products.[22]

In addition to H/D scrambling, complex **1** also reacts with water to give **2**. One plausible route would be the loss of CO_2 from **D** to give complex **G** and subsequent protonation of the platinum center by the protonated pyrazolyl ring yielding complex **2** (Scheme 4). $^{13}CO_2$ was observed in the $^{13}C\{^1H\}$ NMR spectra recorded during the reaction of ^{13}CO-labelled **1**.[20] Although this was found to be a downhill process, the large barrier to **TS(B_2-D)** precludes this route. However, complex **G** can also be reached starting from $\mathbf{E_1}$. Initial rotation of the COOH ligand gives complex $\mathbf{E_2}$; this step is nearly isergonic. Here, the pyrazolyl ring can dissociate and deprotonate the COOH ligand to give the CO_2 complex **F**. Loss of CO_2 from

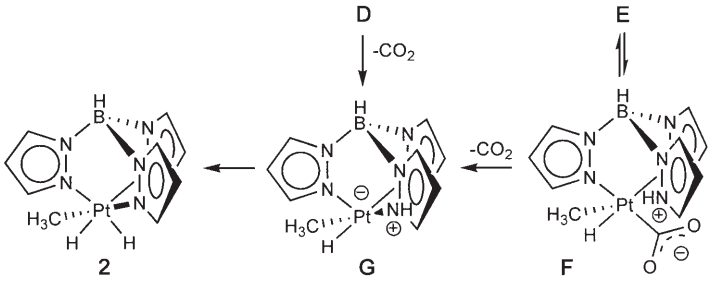

Scheme 4.

F is easy and gives complex **G**. This is a highly exergonic step and only a small barrier (**TS(G-2)**, $\Delta G^{\ddagger}_{298}=12.1$ kcal mol^{-1}) separates **G** from **2**. The barrier to the formation of **2** equates to the overall reaction energy going from $\mathbf{E_1}$ to **F** and is $\Delta G^{\ddagger}_{298}=22.4$ kcal mol^{-1}.

Complex $\mathbf{E_1}$ turns out to be the linchpin in the overall scheme. From here, there are three possible reactions: 1) C–H reductive coupling to give the σ-methane complex $\mathbf{C_2}$; 2) N–H reductive elimination to return to the starting materials $\mathbf{1}+H_2O$; 3) CO_2 deprotonation. The first two are involved in the H/D exchange process while the last leads to the product **2**. The barriers from $\mathbf{E_1}$ for these three reactions are $\Delta G^{\ddagger}_{298}=23.8$, 27.8 and 22.4 kcal mol^{-1}, respectively. These values are far too close to make any definitive statements regarding their relative magnitudes, especially considering the error bars of 3–5 kcal mol^{-1} that even the best DFT method would have. Moreover, a difference of about 1.4 kcal mol^{-1} in barrier height would lead to a difference in reaction rate of one order of magnitude. Nonetheless, the three barriers of similar height explain both the H/D exchange in **1** and the slower conversion of **1** into **2**.

Conclusions

The H/D exchange reaction between **1** and D_2O was found to involve the formation and deprotonation of a sticky σ-methane ligand. Theoretical calculations support such a premise. The efficiency of this nontrivial process can be attributed to the spatial organization of functional groups that operate in concert to activate a water molecule and then achieve a multistep proton walk from water to the uncoordinated pyrazolyl nitrogen atom, to the platinum–methyl bond, and then back again to water by the reverse route.

There are some parallels between the mechanisms of the complexes studied here and Nature's catalytic triad in serine proteases.[1] The spatial orientation of the ligands in complex **1** is important in directing the attack of water on the carbonyl and in transporting the proton around the molecule. The critical role played by the free pyrazolyl nitrogen atom, acting as both base and acid, resembles the dual functionality of the histidine residue in the catalytic triad of natural serine proteases. This machinery highlights the opportunities emerging for the use of biological concepts and strategies in organometallic catalysis. It also underscores the growing evidence that proton transfer processes in aqueous organometallic complexes play crucial roles in biology[41] and medicine.[42]

Experimental Section

General methods: Unless otherwise specified NMR spectra were recorded at room temperature on either a Varian Mercury-300, a Bruker DRX-500 or a Bruker DRX-600 spectrometer. The ^{1}H and ^{13}C NMR signals are reported in ppm downfield from tetramethylsilane and referenced to residual solvent resonances (^{1}H NMR: $\delta=5.32$ ppm for CD_2Cl_2, 4.67 ppm for D_2O/[D_8]THF (1:1) and D_2O/[D_6]acetone (1:1), 3.30 ppm for CD_3OD, 2.04 ppm for [D_6]acetone; ^{13}C NMR: $\delta=53.8$ ppm for CD_2Cl_2, 29.8 ppm for D_2O/[D_6]acetone (1:1)); the chemical shifts are followed in parentheses by multiplicity, coupling constants, *J*, in hertz and integration. Radial chromatography was carried out with a Harrison Research Chromatotron under argon using silica gel plates that were prewashed with deoxygenated eluent saturated with D_2O. Removal of the small amount of protiowater from the eluting solvent (up to 500 mL) was carried out by extraction with D_2O (99.9% D, 3×5 mL). The resulting eluent was further saturated with 5 mL of D_2O during the chromatographic separation. Electrospray mass spectra (ESI-MS) were acquired on a Finnigan LCQ ion-trap mass spectrometer. GC–MS analyses were obtained on a Hewlett-Packard 5971A spectrometer with an electron ionization source. All reactions were conducted in J. Young NMR tubes with resealable Teflon caps. The tubes were pre-silylated with 1,1,1,3,3,3-hexamethyldisilazane and flame-dried under vacuum to avoid any acid-catalyzed hydrophilic reactions. Unless otherwise noted, all manipulations were performed by a combination of standard Schlenk and vacuum-line techniques.[43]

Materials: All deuteriated solvents were purchased from Cambridge Isotope Laboratories and were deoxygenated by bubbling argon through commercially supplied containers. Labeled water, 95.2 at% ^{18}O, was purchased from Rotem Industries, Israel. [^{13}C]Carbon monoxide (99 at% ^{13}C, 99.93 at% ^{16}O) was purchased from Isotec. [D_4]Methane (99 at% D) was purchased from Cambridge Isotope Laboratories. For H/D and ^{16}O/^{18}O exchange reactions, [D_6]acetone, [D_8]THF, CD_2Cl_2, and CD_3CO_2D were dried according to published procedures[44] and vacuum-transferred prior to use. Sephadex LH-20 (Fluka) was used to separate charged species. Tetramethylammonium triflate (Me_4NOTf),[45] which was used as an internal standard in NMR reactions, and compounds **1**,[46] **3**,[47] **4**,[21] **5**,[48] and **6**[20] were prepared according to literature methods.

Synthesis of 7: Complex **1** (122.3 mg, 0.271 mmol) was placed in a Schlenk flask and vacuum-line techniques were followed. Under a positive argon pressure, Me_3OBF_4 (40.1 mg, 0.271 mmol) was added to the reaction flask and Schlenk techniques were performed briefly. CH_2Cl_2 (10 mL, dried over CaH_2) was then added through a cannula and a clear solution resulted within 5 min. The reaction was stirred at room temperature for 6 h under argon. Any insoluble species were then filtered off through a glass-fritted funnel using a cannula under vacuum and dry CH_2Cl_2 (5 mL) was used to rinse the reaction flask and the filter funnel. The solvent of the combined filtrate was removed under vacuum and the solid residue was further dried over P_2O_5 in vacuo to give **7** as a white foamy solid in a quantitative yield (162.0 mg). This complex is somewhat moisture-sensitive and should be stored in a gas-tight desiccator.

^{1}H NMR (CD_2Cl_2): $\delta=8.11$ (d, $J=2.4$ Hz, 1H), 8.10 (d, $J=2.3$ Hz, 1H), 8.06 (d, $J=2.7$ Hz, 1H), 7.93 (d, $J=2.4$ Hz, 1H; $J_{Pt,H}=16.8$), 7.86 (d, $J=2.1$ Hz, 1H; $J_{Pt,H}=10.2$), 7.35 (d, $J=2.7$ Hz, 1H), 6.64 (t, $J=2.4$ Hz, 1H), 6.62 (t, $J=3.0$ Hz, 1H), 6.60 (t, $J=2.4$ Hz, 1H), 3.92 (s, 3H), 1.10 ppm (s, $^2J_{Pt,H}=70.2$ Hz, 3H). ^{1}H NMR ([D_6]acetone): $\delta=8.44$ (d, $J=2.7$ Hz, 1H), 8.32 (d, $J=2.4$ Hz, 1H), 8.30 (d, $J=2.1$ Hz, 1H), 8.20 (d, $J=2.4$ Hz, 1H; $J_{Pt,H}=12.0$), 8.14 (d, $J=2.4$ Hz, 1H; $J_{Pt,H}=17.8$), 7.72 (d, $J=3.3$ Hz, 1H), 6.74 (t, $J=3.0$ Hz, 1H), 6.72 (t, $J=2.7$ Hz, 1H), 6.66 (t, $J=2.4$ Hz, 1H), 4.00 (s, 3H), 1.04 ppm (s, $^2J_{Pt,H}=70.5$ Hz, 3H); ^{13}C NMR (CD_2Cl_2, 75.5 MHz): $\delta=163.34$ ($J_{Pt,C}=1911.6$ Hz, CO), 145.24 ($J_{Pt,C}=35.3$ Hz), 143.17 ($J_{Pt,C}=67.3$ Hz), 141.04 ($J_{Pt,C}=28.2$ Hz), 139.51, 139.10 ($J_{Pt,C}=$

31.7 Hz), 138.85, 108.62 ($J_{Pt,C}$ = 19.6 Hz), 108.28 ($J_{Pt,C}$ = 42.1 Hz), 107.61, 38.88 (N-CH_3), −16.87 ppm ($J_{Pt,C}$ = 527.1 Hz, Pt,CH_3).

Synthesis of 8: The same procedure described previously for the formation of **2** from **1** was followed to generate **8** from **5**.[20] The title complex was isolated by Sephadex LH-20 column chromatography (CD_3OD/CH_2Cl_2 1:2) as an off-white solid in around 60% yield (purity estimated to be 90%).

^{1}H NMR (D_2O/[D_6]acetone 1:1): δ = 9.97 (s, 1H), 8.65 (d, J = 3.0 Hz, 2H), 8.63 (d, J = 3.3 Hz, 1H), 8.28 (d, J = 2.4 Hz, 2H), 8.16 (d, J = 2.2 Hz, 1H), 6.82 (t, J = 2.4 Hz, 2H), 6.77 (t, J = 2.4 Hz, 1H), 1.31 (s, $^2J_{Pt,H}$ = 67.2 Hz, 3H), −18.50 ppm (s, $^1J_{Pt,H}$ = 1275.6).

Synthesis of ^{13}CO-labeled carbonyl complexes 1, 5, 6, and 7: The procedures previously described for the synthesis of the ^{12}C analogues were followed, but with ^{13}C-labeled CO instead of the unlabeled gas.

H/D exchange in complexes 1 and 5

Complex 1: In a typical experiment, a J. Young NMR tube was charged with **1** (6.8 mg, 0.015 mmol) and an internal standard (Me_4NOTf, 0.4 mg) and Schlenk techniques were applied to deoxygenate the solid mixture. The deuteriated solvent (0.8 mL), either D_2O/[D_8]THF (1:1) or D_2O/[D_6]acetone (1:1), was added under argon and the resulting solution was further deoxygenated by two freeze–pump–thaw cycles. The reaction mixture was then kept at room temperature under subdued light, and the progress of the reaction was monitored by ^{1}H NMR spectroscopy. The reaction rate in D_2O/[D_8]THF or in D_2O/[D_6]acetone was found to be quite similar. However, the solubility of product **2** in D_2O/[D_6]acetone (1:1) was only moderate and an appreciable amount of **2** in its crystalline form built up on the wall of NMR tubes. The crystalline **2** was analytically pure, as verified by ^{1}H NMR spectroscopy. During the course of the reaction (up to 14 days), additional methyl signals associated with [D_1]-**1** and [D_2]-**1,** along with **2** and isotopologues of **2**, appeared in the NMR spectrum, while all other proton signals of **1** remained unchanged. Complete deuteriation of the methyl ligand in **1**, as verified by ^{1}H NMR spectroscopy, was achieved by putting the above NMR tube in an oil-bath at 60°C for 30–60 min. The resulting mixture was then subjected to radial chromatography on a Chromatotron (SiO_2, 1 mm, hexane/ethyl acetate (5:2), presaturated with D_2O) under argon to give [D_3]-**1** in 25% yield. By using H_2O instead of D_2O under the above-described conditions, complex [D_1]-**1** reverted back to **1**.

H/D exchange reaction of 1 at 55–60°C: The reaction was conducted in D_2O/[D_8]THF (1:1) and followed by ^{1}H NMR spectroscopy. When the H/D exchange reaction of **1** was carried out in an oil-bath at 55–60°C, a dramatic decrease in integration along with signal distortion in the methyl region was observed within 8 h in the ^{1}H NMR spectrum of the reaction mixture and the above-stated signals had disappeared completely after 24 h. The same isotopologues as described above were identified during the reaction course, but no methane liberation, or that of its isotopologues, could be detected in the NMR spectra. The combined molar ratio of **2** and its isotopologues became dominant within 4 h, as determined by the signals associated with the Tp ligand of **1** and that of **2**, respectively. The combined molar ratio of **1** and [D_1]**1**/[D_2]**1**, which contain detectable methyl protons, decreased over time compared to that of [D_3]-**1**, as determined by the corresponding integrations of the Tp and residual methyl signals in **1**.

H/D exchange reactions of 1 at low temperatures: The reactions were conducted in H_2O/[D_6]acetone (1:1, 0.8 mL) and D_2O/[D_6]acetone (1:1, 0.8 mL) with ^{13}C-labeled complex **1** (20.5 mg, 0.045 mmol) in NMR probes directly and were followed by ^{13}C{^{1}H} NMR spectroscopy for 8 h. In attempts to observe reaction intermediates during the exchange process, the reactions were monitored at 20, 10, 0, and −20°C, respectively, and the ^{13}C{^{1}H} NMR spectra were measured on a Bruker DRX-600 spectrometer using a 30° pulse width, a delay time (d_1) of 0.5 s, a transient number (nt) of 256, and a spectral window of up to 250 ppm. In each reaction, signals associated with the ^{13}C-carbonyl in **1** and $^{13}CO_2$ were observed. Even at −20°C in D_2O/[D_6]acetone (1:1), a trace amount of $^{13}CO_2$ was detected within 2 h. Other signals corresponding to starting material **1** and product **2** were observed and could be clearly identified when a greater number of transients (nt) was used. No other signals, either between 120 and 200 ppm or in other regions, could be detected in the ^{13}C{^{1}H} NMR spectra of the reaction mixtures.

After the above-stated ^{13}C{^{1}H} NMR monitoring period, a ^{1}H NMR spectrum was recorded for each reaction conducted in D_2O/[D_6]acetone (1:1). Small amounts of [D_1]-**1**/[D_1]-**2** were observed for reactions at 0–20°C and the concentrations of **2** and the deuterium-containing isomers of **1** and **2** decreased at lower temperatures. Although the associated signals were weak at lower temperatures, the splitting patterns in most cases could be identified unambiguously and the corresponding chemical shifts matched well the isotope-induced shifts. Note that even at −20°C, a very weak 1:1:1 triplet, corresponding to [D_1]-**1**, was detected.

Complex 5: The same procedure as described above for the H/D exchange reactions of complex **1** was followed. H/D exchange at the methyl group was complete in less than two days. H/D exchange rate in **5** was much faster than in **1**. Likewise, complex **5** reacted faster with water than **1** to give the corresponding dihydridomethylplatinum(IV) complex. Therefore, the rate of actual deuterium incorporation into the methyl group in **1** and **5** was not determined as a result of this competing pathway. A qualitative rate ratio for H/D exchange, based on initial rate measurement by ESI-MS, was found to be over seven-fold greater in **5** than in **1**. Sephadex LH-20 (CD_3OD/CH_2Cl_2 (1:2), dried) was used to isolate [D_3]-**5** under argon and subdued light. However, owing to chromatographical difficulties, [D_3]-**5** was isolated in ≈85% purity based on signal integration of the ^{1}H NMR spectrum (yield undetermined). No further purification was performed. The isolated [D_3]**5** reverted back to **5** on treatment as described above for complex [D_3]-**1**.

During the H/D exchange process in **5**, small amounts of CDH_3 and CD_2H_2, as well as a trace amount of CH_4, were detected. The resulting organometallic complex derived from the loss of methane was not characterized. However, its corresponding protio-complex was identified in the ESI-MS spectrum (1:1 to 3:1 H_2O/acetone) and was consistent with the formula of $[(TpC)Pt(H_2O)(CO_2H)]^+$, as verified by the computer simulation of the isotope distribution pattern. Efforts to unambiguously identify the deuterium-incorporated mass-ion peak in D_2O/[D_6]acetone (1:1–3:1) were not successful, probably because the concentration of the corresponding deuteriated isomer, $[(TpC)Pt(D_2O)(CO_2D)]^+$, was too low in D_2O/[D_6]acetone compared with that in H_2O/acetone as a result of isotope effects. This latter assumption is likely, especially in light of the fact that nucleophilic attack at the carbonyl carbon by $H_2{}^{18}O$ was reported to be a factor of 4.5 faster than that by $D_2{}^{18}O$.[49]

H/D exchange in complexes 3, 4, 6, and 7

Complexes 3 and 4: The same procedure as described above for complex **1** was followed. The resulting samples were then placed in an oil-bath at 55–60°C for two days and the progress of the reactions was monitored by ^{1}H NMR spectroscopy. No detectable change was observed in the methyl signal.

Complex 6: The same procedure as described above for complex **1** was followed. A solution of **6** in D_2O/[D_6]acetone (1:1) was monitored by ^{1}H NMR spectroscopy at room temperature for more than three months under subdued light. No H/D exchange of the methyl ligand was observed. The only change was the appearance of free pyrazole along with a black precipitate containing metallic platinum. The molar ratio of unreacted **6** to pyrazole was 1:3 after 3 months. The presence of pyrazole in the mixture was confirmed by addition of a small amount of an authentic sample of pyrazole to the mixture. The same results were obtained when complex **6** was generated in situ from **1** and HBF_4·Et_2O (1.5 equiv). Likewise, when the reaction of **1** with dry CD_3CO_2D was monitored by ^{1}H NMR spectroscopy, no H/D exchange at the methyl group or methane signal was observed over 3 weeks at room temperature, although trace amounts of free pyrazole were detected.

Complex 7: The same procedure as described above for complex **1** was followed. No H/D exchange at the methyl group or methane liberation was detected in D_2O/[D_6]acetone (1:1) or in CD_2Cl_2 (saturated with D_2O) prior to the complete decomposition of **7** (up to 1 week). Similar to the results observed with **6**, a B–N bond cleavage product was obtained, resulting in the formation of *N*-methylpyrazole. The identity of this latter was confirmed by GC-MS. Other decomposition products were not characterized.

$^{16}O/^{18}O$ exchange in ^{13}CO-labeled complexes 1, 5, 6, and 7: Using complex **1** as an example, a J. Young NMR tube was charged with ^{13}C-labeled **1** (15.8 mg, 0.035 mmol) and Schlenk techniques were applied to deoxygenate the solid. Under argon, [D_6]acetone (0.8 mL) was added, followed by $H_2{}^{18}O$ (100 μL, 5.0 mmol). The resulting mixture was further deoxygenated by two freeze–pump–thaw cycles and the NMR tube was then immediately placed in a methanol/dry-ice bath prior to NMR measurement. The progress of the reaction was monitored by ^{13}C NMR spectroscopy at room temperature using a 30° pulse width and a delay time (d_1) of 0.5 s with the number of transients (nt) set to 32. Owing to other competing reactions, such as CO_2 elimination to produce [$TpPt^{IV}(H)_2Me$] (in the case of **1**) and B–N bond cleavage to produce free pyrazole (in the case of **6**), only relative rates are provided.

Methane ligand exchange reaction in 1: The same procedure as described above for complex **1** was followed. CD_4 (200 mL) was bubbled for 1 min into a solution of **1** (6.8 mg, 0.015 mmol) in H_2O/[D_8]THF (1:1, 0.8 mL) and the reaction was monitored by ^1H NMR spectroscopy, in which a water presaturation program was used. Neither signals associated with free CH_4 and its isotopomers nor deuterium incorporation into the methyl group in **1** could be detected after 2 weeks at room temperature.

Digital resolution for ^1H and ^{13}C NMR spectra in isotope exchange reactions: The isotope exchange reactions were monitored with a Varian NMR spectrometer for which digital resolution is defined as sw/(fn/2), where sw is the sweep width and fn the processing data points. For H/D exchange reactions, a digital resolution of 0.069 Hz per data point along a line broadening of 0.2 Hz was applied to the ^1H FIDs. For $^{16}O/^{18}O$ exchange reactions, a digital resolution of 0.38 Hz per data point along a line broadening of 0.3 Hz was applied to the ^{13}C FIDs.

Computational details: All calculations were carried out using a locally modified version of Gaussian 03, Revision C.01.[50] The modifications include the implementation of new functionals (PW6B95, BMK, and τ-HCTH) and the patch from the research group of Prof. D. Truhlar (University of Minnesota) to the bb95.f that circumvents numerical "0/0" errors.[51] A number of exchange-correlation (XC) functionals were employed. A recent study has shown that for reactions involving late transition metals, the most recommended functional, of the long list tested, was PW6B95, closely followed by PBE0 and B1B95.[40] PW6B95 is a parametrization by Zhao and Truhlar[52] that involves the modified Perdew–Wang exchange functional with Becke's B95 correlation functional; it is classified as a hybrid meta-GGA functional. Other functionals were also used to evaluate the reaction pathway. PBE0 (also known as PBE1PBE) is the hybrid variant, incorporating 25% HF exchange, of the Perdew–Burke–Ernzerhof nonempirical GGA functional.[53] B1B95 combines Becke's GGA exchange functional, 28% HF exchange, and the Becke-95 meta-GGA correlation functional.[54] The Boese–Martin XC functional for kinetics (BMK), a hybrid meta-GGA functional that was developed, in part, by one of the authors for use in studying chemical reactions, was used.[55] Although it has been shown to have exceptional performance for main-group properties and barrier heights (a traditional deficiency of DFT[56,57]), its accuracy for reactions involving transition-metal complexes was less than stellar;[40] nonetheless, it was applied to the reaction system of interest. mPW1K,[58] a high-percentage HF hybrid functional extensively employed in our previous studies, τ-HCTH,[59] and B97-1[60] were also employed.

With these functionals, three basis set–RECP (relativistic effective core potential) combinations were used. The first, denoted SDD, is the combination of the Huzinaga–Dunning double-ζ basis set used for lighter elements and the Stuttgart–Dresden basis set–RECP combination[61] for transition metals. The second, denoted SDB-cc-pVTZ, combines the Dunning cc-pVTZ basis set[62] for the main-group elements and the Stuttgart-Dresden basis set–RECP for transition metals with two *f*- and one *g*-type polarization functions taken from the appendix to reference [63]. Geometry optimizations were carried out using the former basis set whereas the energetics of the reaction were calculated on these geometries with the latter basis set; this level of theory is conventionally denoted as PW6B95/SDB-cc-pVTZ// PW6B95/SDD. Bulk solvent (water) effects were approximated by PW6B95/SDB-cc-pVTZ single-point energy calculations using the conductor screening model (COSMO).[64,65] The identities of the transition states were confirmed by performing intrinsic reaction coordinate (IRC) calculations.[66–68] In certain cases, energies were computed using the SDB-cc-pVDZ basis set. This is similar to its triple-ζ counterpart, but involves the use of the cc-pVDZ basis set for the main-group elements and the SDD basis set–RECP for the transition metals supplemented by a 1*f* polarization function taken as the average of the two *f* functions in the TZ variant.

Acknowledgement

We thank the Skaggs Institute for Chemical Biology for financial support. E.K. thanks the Israel–US Binational Science Foundation and the German–Israeli Project Cooperation (DIP). The ESI-MS spectra were acquired in Dr. Peter Chen's laboratory at the ETH, Zurich (Switzerland). H.C.L. thanks the Skaggs Institute for a fellowship. J.M.L.M. is the Baroness Thatcher Professor of Chemistry and a member ad personam of the Lise Meitner-Minerva Center for Computational Quantum Chemistry. Research at the Weizmann Institute of Science was partly funded by the latter, as well as by the Helen and Martin Kimmel Center for Molecular Design and by the Israel Science Foundation, grant no. 709/05. M.A.I. acknowledges the Feinberg Graduate School for a Ph.D. fellowship.

[1] G. Dodson, A. Wlodawer, *Trends Biochem. Sci.* **1998**, *23*, 347–352.
[2] R. H. Crabtree, *J. Chem. Soc. Dalton Trans.* **2001**, 2437–2450.
[3] S. S. Stahl, J. A. Labinger, J. E. Bercaw, *Angew. Chem.* **1998**, *110*, 2298–2311; *Angew. Chem. Int. Ed.* **1998**, *37*, 2180–2192.
[4] C. Hall, R. N. Perutz, *Chem. Rev.* **1996**, *96*, 3125–3146.
[5] A. E. Shilov, G. B. Shul'pin, *Activation and Catalytic Reactions of Saturated Hydrocarbons in the Presence of Metal Complexes*, Kluwer, Dordrecht, **2000**.
[6] C. L. Hill in *Activation and Functionalization of Alkanes* (Ed.: C. L. Hill), Wiley, New York, **1989**.
[7] B. A. Arndtsen, R. G. Bergman, T. A. Mobley, T. H. Petersson, *Acc. Chem. Res.* **1995**, *28*, 154–162.
[8] A. Sen in *New Approaches in C-H Activation of Alkanes: Applied Homogeneous Catalysis with Organometallic Compounds, 2nd ed., Vol. 3* (Eds.: B. Cornils, W. A. Herrman), Wiley-VCH, New York, **1996**, p. 1226.
[9] N. F. Gol′dshlegger, V. V. Es′kova, A. E. Shilov, A. A. Shteinman, *Russ. J. Phys. Chem.* **1972**, *46*, 785–786.
[10] a) R. A. Periana, D. J. Taube, S. Gamble, H. Taube, T. Satoh, H. Fujii, *Science* **1998**, *280*, 560–564; b) R. A. Periana, O. Mironov, D. Taube, G. Bhalla, C. J. Jones, *Science* **2003**, *301*, 814–818.
[11] A. N. Vedernikov, K. G. Caulton, *Chem. Commun.* **2003**, 358–359.
[12] I. C. M. Wehman-Ooyevaar, D. M. Grove, P. De Vaal, A. Dedieu, G. van Koten, *Inorg. Chem.* **1992**, *31*, 5484–5493.
[13] For the acidity of metal hydrides, see: S. S. Kristjánsdóttir, J. R. Norton in *Transition Metal Hydrides: Recent Advances in Theory and Experiment* (Ed.: A. Dedieu), VCH, New York, **1992**, p. 309.
[14] R. H. Crabtree, P. E. M. Siegbahn, O. Eisenstein, A. L. Rheingold, T. F. Koetzle, *Acc. Chem. Res.* **1996**, *29*, 348–354.
[15] R. H. Crabtree, *Angew. Chem.* **1993**, *105*, 828–845; *Angew. Chem. Int. Ed. Engl.* **1993**, *32*, 789–805.
[16] D. M. Heinekey, W. J. Oldham, Jr., *Chem. Rev.* **1993**, *93*, 913–926.
[17] K.-T. Smith, M. Tilset, R. Kuhlman, K. G. Caulton, *J. Am. Chem. Soc.* **1995**, *117*, 9473–9480.
[18] J. Huhmann-Vincent, B. L. Scott, G. J. Kubas, *J. Am. Chem. Soc.* **1998**, *120*, 6808–6809.
[19] D.-H. Lee, B. P. Patel, E. Clot, O. Eisenstein, R. H. Crabtree, *Chem. Commun.* **1999**, 297–298.
[20] A. Haskel, E. Keinan, *Organometallics* **1999**, *18*, 4677–4680.
[21] a) H. C. Lo, A. Haskel, M. Kapon, E. Keinan, *J. Am. Chem. Soc.* **2002**, *124*, 3226–3228; b) H. C. Lo, A. Haskel, M. Kapon, E. Keinan, *J. Am. Chem. Soc.* **2002**, *124*, 12626.

[22] M. A. Iron, H. C. Lo, J. M. L. Martin, E. Keinan, *J. Am. Chem. Soc.* **2002**, *124*, 7041–7054.
[23] For an intramolecular hydride walk, see: D. B. Grotjahn, H. C. Lo, *J. Am. Chem. Soc.* **1996**, *118*, 2097–2098.
[24] a) When the reaction was conducted in H_2O/acetone (1:1), the conversion of **1** into **2** was completed in 24 h (ref. [20]). However, when D_2O was used, the reaction was significantly slower as shown. As D_2O is a reactant, a primary kinetic isotope effect would be expected. b) When the reaction was carried out in an oil bath at 55–60 °C, a dramatic decrease in the integration along with signal distortion in the methyl region was observed within 8 h, and all the methyl signals had completely disappeared after 24 h.
[25] D. J. Darensbourg, R. A. Kudaroski, *Adv. Organomet. Chem.* **1983**, *22*, 129–168.
[26] Indirect evidence for the existence of a methane ligand was observed in the case of **5**, a cationic isoelectronic analogue of **1** (see text).
[27] D. J. Darensbourg, B. J. Baldwin, J. A. Froelich, *J. Am. Chem. Soc.* **1980**, *102*, 4688–4694.
[28] N. Grice, S. C. Kao, R. Pettit, *J. Am. Chem. Soc.* **1979**, *101*, 1627–1628.
[29] C. P. Casey, M. A. Andrews, J. E. Rinz, *J. Am. Chem. Soc.* **1979**, *101*, 741–743.
[30] P. E. Rush, J. D. Oliver, *J. Chem. Soc., Chem. Commun.* **1974**, 996.
[31] S. Reinartz, P. S. White, M. Brookhart, J. L. Templeton, *Organometallics* **2000**, *19*, 3854–3866.
[32] S. Reinartz, M.-H. Baik, P. S. White, M. Brookhart, J. L. Templeton, *Inorg. Chem.* **2001**, *40*, 4726–4732.
[33] P. E. M. Siegbahn, R. H. Crabtree, *J. Am. Chem. Soc.* **1996**, *118*, 4442–4450. Although a definitive difference cannot be concluded in Shilov's platinum system, deprotonation of a σ-methane ligand was suggested as palladium and mercury analogues clearly proceed by this route.
[34] The process described is the reverse step of the formation of a CH_4 ligand. From the viewpoint of microreversibility, both forward and backward reactions should follow the same pathway in our system. It has been suggested that deprotonation of a CH_4 ligand is best described as a σ-bond metathesis step.[33]
[35] K. Mylvaganam, G. B. Bacskay, N. S. Hush, *J. Am. Chem. Soc.* **2000**, *122*, 2041–2052.
[36] J. P. Collman, L. S. Hegedus, J. R. Norton, R. G. Finke, *Principles and Applications of Organotransition Metal Chemistry, 2nd ed.*, University Science Books, Mill Valley, California, **1987**, p. 88.
[37] D. J. Darensbourg, *J. Organomet. Chem.* **1979**, *174*, C70–C76.
[38] I. C. M. Wehman-Ooyevaar, D. M. Grove, H. Kooijman, P. van der Sluis, A. L. Spek, G. van Koten, *J. Am. Chem. Soc.* **1992**, *114*, 9916–9924. For the X-ray structure of the stated zwitterionic complex and discussion of the N^+–H···Br–Pt^{II-} electrostatic interaction, see p. 9922 therein.
[39] Selected bond distances for the N^+–H···Br–Pt^{II-} zwitterionic complex [Å]: Pt···H 2.446, Br···H 2.486, N···H 0.98. Selected bond distances [Å] for the N^+–H···Pt^{II-} zwitterionic complex: Pt···H 2.11, N···H 0.88.[38]
[40] M. M. Quintal, A. Karton, M. A. Iron, A. D. Boese, J. M. L. Martin, *J. Phys. Chem. A* **2006**, *110*, 709–716.
[41] K. W. Kramarz, J. R. Norton, *Prog. Inorg. Chem.* **1994**, *42*, 1–65.
[42] T. W. Hambley, A. R. Jones, *Coord. Chem. Rev.* **2001**, *212*, 35–59.
[43] D. F. Shriver, M. A. Drezdzon, *The Manipulation of Air-Sensitive Compounds, 2nd ed.*, Wiley, New York, **1986**.
[44] W. L. F. Armarego, D. D. Perrin, *Purification of Laboratory Chemicals, 4th ed.*, Pergamon Press, Oxford, **1997**.
[45] H. C. Lo, C. Leiva, O. Buriez, J. B. Kerr, M. M. Olmstead, R. H. Fish, *Inorg. Chem.* **2001**, *40*, 6705–6716.
[46] H. C. Clark, L. E. Manzer, *Inorg. Chem.* **1974**, *13*, 1996–2004.
[47] A. Haskel, E. Keinan, *Tetrahedron Lett.* **1999**, *40*, 7861–7865.
[48] H. C. Clark, M. A. Mesubi, *J. Organomet. Chem.* **1981**, *215*, 131–138. Silver triflate was used in our study.
[49] D. J. Darensbourg, J. A. Froelich, *J. Am. Chem. Soc.* **1977**, *99*, 5940–5946, and ref. [27] therein.
[50] Gaussian 03, Revision C.01, M. J. Frisch, G. W. Trucks, H. B. Schlegel, G. E. Scuseria, M. A. Robb, J. R. Cheeseman, J. A. Montgomery, Jr., T. Vreven, K. N. Kudin, J. C. Burant, J. M. Millam, S. S. Iyengar, J. Tomasi, V. Barone, B. Mennucci, M. Cossi, G. Scalmani, N. Rega, G. A. Petersson, H. Nakatsuji, M. Hada, M. Ehara, K. Toyota, R. Fukuda, J. Hasegawa, M. Ishida, T. Nakajima, Y. Honda, O. Kitao, H. Nakai, M. Klene, X. Li, J. E. Knox, H. P. Hratchian, J. B. Cross, C. Adamo, J. Jaramillo, R. Gomperts, R. E. Stratmann, O. Yazyev, A. J. Austin, R. Cammi, C. Pomelli, J. W. Ochterski, P. Y. Ayala, K. Morokuma, G. A. Voth, P. Salvador, J. J. Dannenberg, V. G. Zakrzewski, S. Dapprich, A. D. Daniels, M. C. Strain, O. Farkas, D. K. Malick, A. D. Rabuck, K. Raghavachari, J. B. Foresman, J. V. Ortiz, Q. Cui, A. G. Baboul, S. Clifford, J. Cioslowski, B. B. Stefanov, G. Liu, A. Liashenko, P. Piskorz, I. Komaromi, R. L. Martin, D. J. Fox, T. Keith, M. A. Al-Laham, C. Y. Peng, A. Nanayakkara, M. Challacombe, P. M. W. Gill, B. Johnson, W. Chen, M. W. Wong, C. Gonzalez, J. A. Pople, Gaussian, Inc., Wallingford, CT, **2004**.
[51] Y. Zhao, D. G. Truhlar, *J. Chem. Theory Comput.* **2005**, *1*, 415–432.
[52] Y. Zhao, D. G. Truhlar, *J. Phys. Chem. A* **2005**, *109*, 5656–5667.
[53] J. P. Perdew, K. Burke, M. Ernzerhof, *Phys. Rev. Lett.* **1996**, *77*, 3865–3868.
[54] A. D. Becke, *J. Chem. Phys.* **1996**, *104*, 1040–1046.
[55] A. D. Boese, J. M. L. Martin, *J. Chem. Phys.* **2004**, *121*, 3405–3416.
[56] J. Baker, J. Andzelm, M. Muir, P. R. Taylor, *Chem. Phys. Lett.* **1995**, *237*, 53–60.
[57] J. L. Durant, *Chem. Phys. Lett.* **1996**, *256*, 595–602.
[58] B. J. Lynch, P. L. Fast, M. Harris, D. G. Truhlar, *J. Phys. Chem. A* **2000**, *104*, 4811–4815.
[59] A. D. Boese, N. C. Handy, *J. Chem. Phys.* **2002**, *116*, 9559–9569.
[60] F. A. Hamprecht, A. J. Cohen, D. J. Tozer, N. C. Handy, *J. Chem. Phys.* **1998**, *109*, 6264–6271.
[61] "Effective Core Potentials": M. Dolg in *Modern Methods and Algorithms of Quantum Chemistry, Vol. 1* (Ed.: J. Grotendorst), John von Neumann Institute for Computing, Jülich, **2000**, pp. 479–508.
[62] T. H. Dunning, Jr., *J. Chem. Phys.* **1989**, *90*, 1007–1023.
[63] J. M. L. Martin, A. Sundermann, *J. Chem. Phys.* **2001**, *114*, 3408–3420.
[64] A. Klamt, G. Schürmann, *J. Chem. Soc., Perkin Trans. 2* **1993**, 799–805.
[65] C. J. Cramer, *Essentials of Computational Chemistry: Theories and Models*, Wiley, Chichester, **2002**, pp. 347–383.
[66] K. Fukui, *Acc. Chem. Res.* **1981**, *14*, 363–368.
[67] C. Gonzalez, H. B. Schlegel, *J. Chem. Phys.* **1989**, *90*, 2154–2161.
[68] C. Gonzalez, H. B. Schlegel, *J. Phys. Chem.* **1990**, *94*, 5523–5527.

Received: May 22, 2006
Published online: January 19, 2007

